ELSEVIER

Dyes and Pigments 43 (1999) 7–14

DYES and PIGMENTS

Topochemical photoreaction of self-assembled styryldicyanopyrazine dyes and their solid state spectral properties☆

Jae Hong Kim[a], Yasuteru Tani[a], Masaru Matsuoka[b], Koushi Fukunishi[a,] *

[a]*Department of Chemistry and Materials Technology, Kyoto Institute of Technology, Matsugasaki, Sakyo, Kyoto 606-0962, Japan*
[b]*Laboratory of Material Science, Kyoto Women's University, Imakumano, Higashiyama, Kyoto 605-8501, Japan*

Received 25 November 1998; accepted 14 December 1998

Abstract

The selective topochemical photoreaction of styryldicyanopyrazine dyes was studied, and showed an anti head-to-tail type cyclobutane ring. Substituent effects were correlated with the self-assembling characteristics of the reactants. The solid state photoreactions were explained in terms of the specific crystal lattice packing of the molecules and their dynamic performance in the crystal structures with the aid of their X-ray crystal analyses. Absorption and fluorescence spectral properties in the solid state were evaluated by the self-assembling characteristics and the intermolecular π–π interactions in the solid state. © 1999 Elsevier Science Ltd. All rights reserved.

Keywords: Styryldicyanopyrazine dyes; Topochemical photoreaction; X-ray crystal analysis; Self-assembling; Solid state spectra

1. Introduction

Almost all of functionalities of organic dye molecules are induced by the π-electron oriented intermolecular interaction in the aggregates. This causes strong molecular stackings which are very significant with respect to special functionalities of the solid state [1,2]. The solid state chemistry of organic materials is of current interest in order to correlate their functionality with the molecular stacking behavior in aggregates [3] for functional materials such as organic nonlinear optical materials, organic photoconductors [4] and emitters for electroluminescence. A dye molecule has the large π-conjugated planar structure and becomes a valuable candidate for organic functional materials [5]. We have reported that the self-assembling characteristics of some naphthoquinone dyes consisting of a strong three dimensional molecular stacking show a large 3rd order nonlinear optical susceptibility [6,7].

In the solid state intermolecular photodimerization, it is generally accepted that the crystal structure and the distance between the reactive centers determine the stereoselectivity and reactivity, because of the limited motions of molecules compared with those in solution. This concept, i.e. topochemical principles [8], was first suggested by

---

☆ The full X-ray structure report is available on request from the corresponding author.

* Corresponding author. Tel.: +81-75-724-7515; fax: +81-75-724-7580.

E-mail address: fukunishi@chem.kit.ac.jp (K. Fukunishi)

PII: S0143-7208(99)00029-7

Schmidt [9], and a number of investigations concerning solid state photocycloaddition were conducted, which led to the formulation of Schmidt's criterion [10–14] viz., the double bonds should be oriented approximately parallel and their distance should be no greater than 4.1 Å. This rule, however, has several exceptions [15–17]. Recent studies on the photodimerization of olefinic crystals have revealed that the reactivity of crystals is related to the free space around the reaction site in the crystal lattice. The terms "reaction cavity" and "steric compression control" have been proposed to explain irregular solid state photochemical reactions [18–21]. A number of lattice energy calculations were carried out to evaluate the reactivity of olefinic crystalline compounds, and these were in agreement with the experimental observations [22,23].

In this paper, we intend to confirm the specific steric compression effects that control the reactivities and physical properties of the reactants in the solid state. This concept is useful in understanding most photochemical behaviors of olefinic compounds in the solid state.

Photocycloadditions of phenylethenyldicyanopyrazines were carried out in solution, the vapor deposited thin films, and in single crystals. The differences in the crystal structures strongly influenced the solid state photodimerizations, which were studied by X-ray crystal analysis. The self-assembling characteristics of chromophores were also correlated with their absorption and fluorescence spectra in the solid state.

2. Results and discussion

2.1. Photoreaction of styryldicyanopyrazines **1a–1g**

Photoreactions of **1** were carried out in benzene solution, vapor deposited thin film and single crystals (Scheme 1). A benzene solution of **1** was irradiated by UV light at 366 nm for 20 h to yield the corresponding *cis*-isomer **2** (95–70%) and the photodimer **3** (5–30%) in a conversion of 97–65% (Table 1). The anti head-to-tail dimerized structure of **3** was confirmed by ^{1}H NMR and mass spectroscopy. The photoreactions of **1a–1g** occurred in high conversion regardless of variations of the ratio of **2**:**3**. On the other hand, the solid photoreaction of **1** showed somewhat different reactivity, depending on the substituent in **1**.

The photoreactions of the vapor deposited thin films of **1a–1c** gave the corresponding photodimers **3a–3c** in high yield. However, the photoreactions of **1d** ($R^1 = OBu$, $R^2 = R^3 = H$) and of **1f** ($R^1 = Ph$, $R^2 = H$, $R^3 = Me$) did not occur. Interestingly, **1e** and **1g** turned into the photodimers **3e** and **3g**, in poor and moderate yields respectively, in spite of their having a bulky *t*-butyl group. Unreacted **1g** was quantitatively recovered. The corresponding *cis*-isomer **2** was not detected on photoirradiation in the vapor deposited thin film of **1**.

Similarly, when single crystals of **1a** and **1g** were irradiated by UV light at 366 nm for 10 h, the photodimer having an anti head-to-tail form **3a** was obtained in high yield (90%), whereas **1g** gave

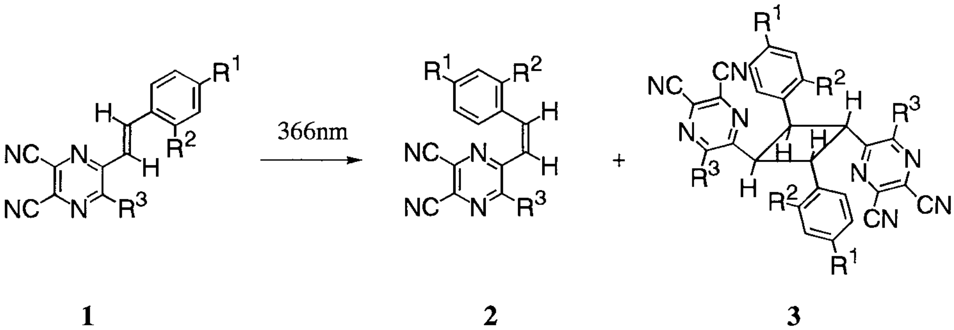

Scheme 1.

Table 1
Photoreaction of **1a**–**1g** in benzene and the vapor deposited thin film

				Benzene solution			Vapor deposited thin film
	R^1	R^2	R^3	Conversion (%)	**2** (%)	**3** (%)	**3** (%)
1a	H	H	H	78	82	18	100
1b	OMe	H	H	70	85	15	96
1c	H	OMe	H	70	70	30	76
1d	OBu(n)	H	H	65	70	30	0
1e	Bu(tert)	H	Me	77	92	8	5
1f	Ph	H	Me	97	95	5	0
1g	Bu(tert)	H	Et	81	85	15	37

the dimer **3g** in 17% yield. The *cis*-isomers **2a** and **2g** were not obtained.

2.2. Solid state photoreaction

The solid state photoreaction is influenced both by the crystal structure and the distance between the reactive centers which determine the reactivity and the stereoselectivity, because of the limited motion of the molecules [8]. The X-ray crystal structures of **1a** and **1g** were examined to study the relationship between the molecular stacking and the reactivity. The molecular structures of **1a** and **1g** are shown in Fig. 1. The X-ray crystal analysis of **1a** reveals the planar layered structure with interlayer distances of 3.33 Å (Fig. 2). Each molecule is oriented in the same line of direction to the b-axis, and the next nearest lines are oriented in the reverse direction. Alternative orientations of the each line are observed in the same plane.

Molecular pairing of **1a** is observed between the interlayered structures, and two molecules are completely overlapped, with the reverse direction in each of the paired molecules. The reactive double bonds are in parallel and the distances of the corresponding carbon atoms for cycloaddition are 3.65 and 3.66 Å (Fig. 3). This would be well reproduced in the photoreaction in the vapor deposited thin film of **1a**. There is no doubt that the photoreaction product **3a** in the solid state is the anti head-to-tail dimer. The photodimerization of **1b** and **1c** gave the similar results to that of **1a**, suggesting similar molecular packings (Table 1).

On the other hand, the photoreaction of **1g**, which contains a bulky *t*-butyl group, reduced considerably the yield of **3g**, compared with that of **1a–1c** in the solid state, indicating an intrinsic reactivity of this compound in the solid state. The X-ray crystal analysis of **1g** reveals that each molecule is oriented in a zig-zag orientation to the *a*-axis and in the diverse direction to the *b*-axis in a plane, due to the steric repulsion of the bulky *t*-butyl group. Molecular pairing occurs in the reverse direction between the interlayer structures, and the layered distance is found to be 3.54 Å (Fig. 3). However, steric repulsion between the *t*-butyl group and the 5-cyano group causes a considerable slant of the overlap in the molecular pairing. The intermolecular distances between the corresponding carbon atoms of the reactive double bonds in the pair are 4.64 and 4.65 Å, respectively (Fig. 3).

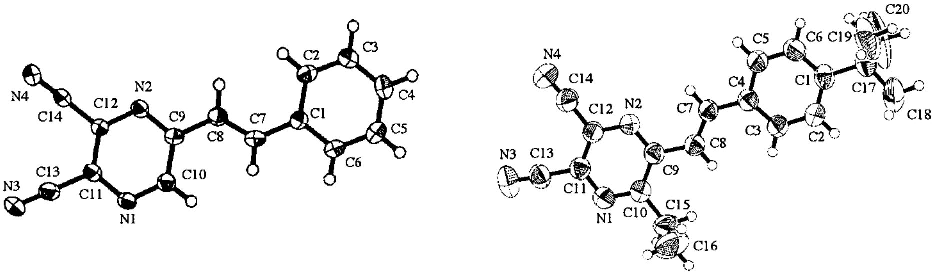

1a **1g**

Fig. 1. Molecular structure of **1a** and **1g**.

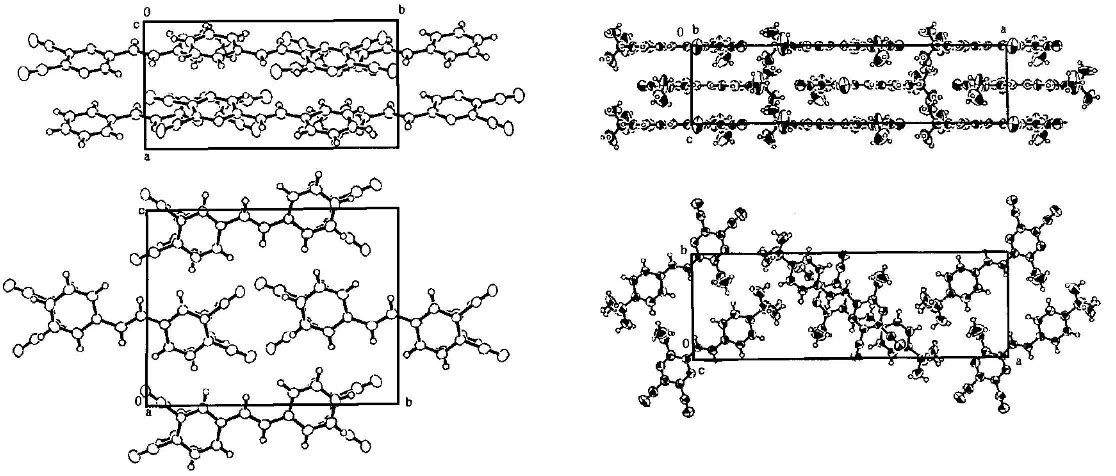

1a **1g**

Fig. 2. The molecular packing arrangement of **1a** and **1g**; interlayer structure (top) and the overlapped pair (bottom).

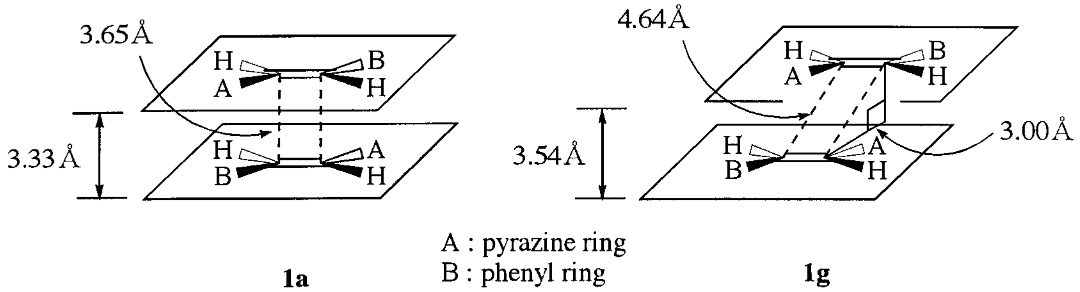

Fig. 3. Differences in packing mode of the double bonds, **1a** and **1g** in the crystals.

It is suggested that in **1g** the reactive pair should be slid about 3 Å in the same plane to overlap, and to facilitate photocycloaddition. It is likely that such a movement will give a moderate yield of **3g**, regardless of a steric hindrance, due to interaction between the *t*-butyl and cyano groups in the pairs.

Similar solid state photodimerization of 4-formyl cinnamic acid has been reported to proceed, in spite of the long distances of 4.8 Å between the reactive double bonds [24]. On the other hand, the crystal of 4,4,8α-trimethyl-8aβ-carbomethoxy-4aβ,5,8,8α-tetrahydro-1(4H)-naphthalene-1-one was inert to photodimerization. The molecules were ideally arranged to undergo photodimerization, and the reactive enone double bonds were parallel and the distance of center-to-center in double bonds was 3.79 Å [19]. It has been explained by Scheffer et al. that further movement of enone molecules toward each other to result in overlap was completely prohibited, owing to the mutual sterical repulsion, called specific crystal lattice packing effects (steric compression control). “Topochemically allowed molecular movement” [18] in the “reaction cavity” [20] or “free space” [21] around the reaction site are a prerequisite for crystal reactivity. It is of interest to note that the photodimerization of **1g** proceeds with topochemically allowed molecular movement, accompanied by a molecular movement of 1.5 Å in each other to prevent possible *t*-butyl—cyano group repulsion. However, the lower photoreactivity of **1g** is due to the lower overlap of the double bond, because the repulsion of the *t*-butyl group and the cyano group may make it difficult to move the molecules to each other for a paired structure on photocycloaddition. In contrast, solid state photoreactions of **1d** and **1f** with large substituents did not occur; such structures inhibit the overlap of reactive double bonds, because of the steric compression in the paired structure. Pertinent X-ray crystal data of **1d** and **1f** to clarify such a mechanism are not yet available. However, it may be concluded that the solid state photocycloaddition of styryldicyanopyrazine dyes, especially **1d**–**1g**, proceeds with the allowed movement of molecules in the crystal lattice, which should be considered with respect to reaction cavity, steric compression and dynamic preformance in the crystals.

2.3. Solid state absorption and fluorescence properties of styryldicyanopyrazines

The solid state absorption and fluorescence spectra of organic chromophores are well correlated with their molecular packing arrangements in aggregates or crystals [1,3,25]. We were also expecting a characteristic spectral change in intensity and wavelength of aggregates and crystals of organic dye materials. The differences in the molecular stacking of **1a** and **1g** depended on the steric parameters of the substituents, and were influenced both on their reactivities and spectral properties. Absorption and fluorescence spectra of **1a**–**1g** in solution and in their vapor deposited thin film are summarized in Table 2.

Compounds **1a**–**1g** had a single absorption peak in the range of 371–411 nm and showed an intensive fluorescence at 447–504 nm (Ex = 365 nm) in solution. The vapor deposited thin film of **1a**, **1b** and **1c** showed a large shoulder peak or split peaks in their absorption spectra and very weak fluorescence. On the other hand, thin films of **1d**–**1g** having bulky substituents showed a small shoulder peak in the absorption spectra and intensive fluorescence. Various absorption and fluorescence changes in λ_{max} and F_{max} were observed between the solution and thin film spectra of **1a**–**1g**, and there were especially distinct characteristics in the fluorescence intensity of thin films of **1a** and **1g**. Although fluorescence of the **1a** film was quenched completely, the **1g** film emitted a strong fluorescence at 460 nm. Compounds in Table 2 are grouped into two types, viz., **1a**–**1c** and **1d**–**1g**, depending on the fluorescence intensity of their evaporated thin films.

Table 2
Absorption and fluorescence spectra of **1** in solution and the vapor deposited thin film

	Chloroform solution			Vapor deposited thin film		Δ	
	λ_{max}	F_{max}	ss^a	λ_{max}	F_{max}	$\Delta\lambda^b$	ΔF^c
1a	371	447	76	337, 419^d	465 (w)^e	48	18
1b	407	500	93	407, 427^f, 457^f	489 (w)^e	0	−11
1c	397	485	88	408,440^f	506 (w)^e	11	21
1d	411	504	93	397, 450^g	496 (i)^h	−14	−8
1e	387	482	95	373, 415^g	483 (i)^h	6	20
1f	397	476	79	367^d, 430^d, 453	515 (i)^h	55	39
1g	384	456	72	373, 415^g	460 (i)^h	−11	4

[a] Stocks shift.
[b] $\Delta\lambda = \lambda_{max}$ (film)–λ_{max} (soln).
[c] $\Delta F = F_{max}$ (film)–F_{max} (soln).
[d] Split peak.
[e] Very weak fluorescence.
[f] Large shoulder peak.
[g] Small shoulder peak.
[h] Intensive fluorescence.

The inherent overlapping of the π-electrons in the paired structure are strongly correlated with the solid state spectra [26]. An almost complete molecular pairing in the crystal structure of **1a** was observed in the distances of 3.33 Å between the interlayers, and the π-orbitals of each molecules were entirely overlapped with reverse direction to cancel the dipole moment in the paired structure. Such a paired molecular stacking structure is required for effective fluorescence quenching, as well as for the solid state photoreaction of **1a**.

The difference in the fluorescence characteristics between **1a** and **1g** would be due to the variable molecular overlap of their π-electrons; sufficient overlapping effectively quenches the solid state fluorescence, and a lower overlapping has little effect on the fluorescence. Although the mechanism of the fluorescence quenching mechanism in the solid state is not yet fully apparent, fluorescence quenching accompanying increase of concentration and the formation of aggregates is well known. Alternatively, the degree of overlapping of the π-electrons with neighbouring molecules, and their interlayer distances, may significantly influence the solid state fluorescence.

3. Experimenral

3.1. General

Characterization of all compounds was carried out by general procedures using the following equipment; M.p.: Yanagimoto micro melting point apparatus, uncorrected; ^{1}H NMR spectra: FT-NMR QE 300 MHz Shimadzu spectrometer; chemical shifts in ppm with reference to TMS, mass spectra: M-80 B Hitachi mass spectrometer. UV-Vis spectra: U-3410 Hitachi spectrophotometer.

3.2. General procedure for **1a–1g**

The appropriate benzalacetones were prepared by aldol condensation of benzaldehydes with acetone in alkaline medium. The benzalacetones were oxidized with selenium dioxide in dioxane, and the reaction mixtures were filtered and cooled to room temp. Diaminomalonitrile was added to the filtrate, which was then refluxed for 5 h to give **1a**–**1d**. The formation of 3-alkyl substituted-2-styryl dicyanopyrazines **1e**–**1g** via Wittig reaction has been previously reported [27].

3.3. Preparation of evaporated thin films and single crystals

Compounds **1** were evaporated vertically from a heated plate onto a glass or quartz plate under about 5×10^{-6} Torr by using a vapor deposition apparatus. The distance between the sample and plate, and also the evaporating temperature, were controlled depending on the property of **1**. A single crystal **1a** or **1g** was grown in chloroform by slow evaporation of the solvent. After several days, yellow crystals of **1a** or **1g** were separated, collected and used for photoreaction and X-ray crystal analysis.

3.4. X-ray crystal analysis date of **1a** and **1g**

1a; Chemical formula: $C_{14}H_8N_4$; formula weight: 232.24; crystal system: monoclinic; lattice parameters: a = 7.317(2) Å, b = 14.155(8) Å, c = 11.061(3) Å, β = 94.54(3), V = 1140.3(7) Å^3: standard deviation 1.48; space group: $P2_1/c$; Z: 4; μ: 0.86; No. of reflection: 2278; R: 0.056; Rw: 0.072

1b; Chemical formula: $C_{20}H_{20}N_4$; formula weight: 316.40; crystal system: orthorhomobic; lattice parameters: a = 27.772(7) Å, b = 9.441(2) Å, c = 7.012(9) Å, V = 1838.4(5) Å^3: standard deviation 1.89; space group: $Pna2_1$; Z: 4; μ: 5.45; No. of reflection: 1669; R: 0.046; Rw: 0.071.

3.5. General procedure of photoreaction in solution

Compounds **1** (1 mmol) were dissolved in benzene (20–40 ml) and irradiated by UV light (366 nm) at room temp for 20 h under N_2 atmosphere. The reaction mixture was evaporated in vacuo at room temp. The products were separated by column chromatography using dichloromethane as eluent.

3.6. Photoreaction in single crystals of **1a** and **1g**

Finely powdered single crystals of **1a** was irradiated directly with a mercury arc lamp for 10 h under a N_2 atmosphere. The products were separated by column chromatography using dichloromethane as eluent to give **3a** (90%) together with unreacted **1a** (10%), respectively. Similarly **3g** was obtained in 17% yield, and **1g** (83%) was recovered. These yields were estimated from ^{1}H NMR measurements.

3.7. Characterization of **1**

1a; mp: 233–234°C; δ_H (CDCl$_3$) 8.82(1H, s), 8.04(1H, d, J = 15.3), 7.67–7.64(2H, m), 7.47–7.40(3H, m), 7.19(1H, d, J = 15.3); EA, Calcd.: $C_{14}H_8N_4$ (C, 72.40; H, 3.47; N, 24.12) Found: (C, 72.53; H, 3.58; N, 24.20); m/z (M$^+$): 232.

1b; mp: 216–217°C; δ_H (CDCl$_3$) 8.75(1H, s), 8.00(1H, d, J = 15.6), 7.61(2H, d, J = 8.6), 7.03(1H, d, J = 15.6), 6.97(2H, d, J = 8.6), 3.86(3H, S); EA, Calcd.: $C_{15}H_{10}N_4O$ (C, 68.69; H, 3.84; N, 21.36) Found: (C, 68.66; H, 3.95; N, 21.35); m/z (M$^+$): 262.

1c; mp: 219–220°C; δ_H (CDCl$_3$); 8.81(1H, s), 8.31(1H, d, J = 15.9), 7.62(1H, dd, J_1 = 7.8, J_2 = 1.8), 7.42(1H, ddd, J_1 = 8.7, J_2 = 7.5, J_3 = 1.8), 7.30(1H, d, $J=15.9$), 7.03(1H, *t*, $J=7.5$), 6.98(1H, d, $J=8.4$), 3.97(3H, s), EA, Calcd.: $C_{15}H_{10}N_4O$ (C, 68.69; H, 3.84; N, 21.36) Found: (C, 68.44; H, 3.93; N, 21.24); *m*/*z* (M^+): 262

1d; mp: 153°C; δ_H ($CDCl_3$) 8.74(1H, s), 7.99(1H, d, $J=15.8$), 7.59(2H, d, $J=8.4$), 7.01(1H, d, $J=15.8$), 6.95(2H, d, $J=8.4$), 4.03(2H, t, $J=6.2$), 1.80(2H, quint, $J=6.2$), 1.53(2H, six, $J=7.2$), 0.99(3H, t, $J=7.2$); EA, Calcd.: $C_{18}H_{16}N_4O$ (C, 71.04; H, 5.30; N, 18.41) Found: (C, 71.05; H, 5.38; N, 18.41); *m*/*z* (M^+): 304

1e; mp: 239°C; δ_H ($CDCl_3$) 8.12(1H, d, $J=15.6$), 7.60(2H, d, $J=8.1$), 7.47(2H, d, $J=8.4$), 7.19(1H, d, $J=15.6$), 2.79(3H, S), 1.35(9H, s); EA, Calcd.: $C_{19}H_{18}N_4$ (C, 75.47; H, 6.00; N, 18.53) Found: (C, 75.64; H, 6.10; N, 18.19); *m*/*z* (M^+): 302

1f; mp: 284–286°C; δ_H ($CDCl_3$) 8.17(1H, d, $J=15.3$), 7.76–7.63(6H, m), 7.50–7.39(3H, m), 7.26(1H, d, $J=15.3$), 2.82(3H, s); EA, Calcd.: $C_{21}H_{14}N_4$ (C, 78.24; H, 4.38; N, 17.38) Found: (C, 77.64; H, 4.57; N, 17.17); *m*/*z* (M^+): 322

1g; mp: 205°C; δ_H ($CDCl_3$) 8.13(1H, d, $J=15.3$), 7.61(2H, d, $J=8.4$), 7.48(2H, d, $J=8.4$), 7.23(1H, d, $J=15.3$), 3.10(2H, q, $J=7.5$), 1.40(3H, t, $J=7.5$), 1.36(9H, s); EA, Calcd.: $C_{20}H_{20}N_4$ (C, 75.92; H, 6.37; N, 17.71) Found: (C, 75.70; H, 6.47; N, 17.37); *m*/*z* (M^+): 316

3.8. Stereochemical assignments of **2** *and* **3**

The assignment of **2a**–**2g** was conducted using ^1H NMR, which showed typical *cis*-coupling ($J=12$ Hz) for the proton in the olefinic moiety with respect to that of the *trans* form ($J=15$ Hz). The stereochemical assignment of **3a** was evaluated by its mass spectrum, which shows *m*/*z* 464 (M^+) and 232 ($M^+/2$), while the peak corresponding to asymmetric cleavage of the cyclobutane, moiety, usually observed in similar noncentrosymmetric 1,2- or 1,3-diaryl-disubstituted cyclobutanes, was absent. The ^1H NMR spectrum showed a singlet for 2 protons attached to the pyrazine ring at δ 8.51 ppm, and two multiplets for 10 aromatic protons on the cyclobutane ring (centered at δ 7.22 and 7.10 ppm). Two sets of doublet of doublets for the two paired protons on the cyclobutane ring were observed at δ 5.05 and 4.85 ppm ($J_1=10.2$ Hz, $J_2=7.2$ Hz), typical for a symmetrical *trans*, *trans*-AA′BB′ pattern. From these results, **3a** has an anti head-to-tail configuration, which is well in accord with the crystal structure of the paired **1a**. The ^1H NMR spectra of the cyclobutane ring in **3b**–**3g** showed a similar pattern to that of **3a**, and was assigned an anti head-to-tail configuration.

References

[1] Kazmaier PM, Hoffmann R. A theoretical study of crystallochromy. Quantum interference effects in the spectra of perylene pigments. J Am Chem Soc 1994;116:9684–91.

[2] Inabe T, Mitsuhashi T, Maruyama Y. Charge transfer complexes based on the twin-TCNQ-type acceptor 11,11,12,12,13,13,14,14-octacyano-1,4:5,8-anthradiquinotetramethane (OCNAQ). Bull Chem Soc Jpn 1998;61:4215–24.

[3] Dahne L. Self-organization of polymethine dyes in thin solid layers. J Am Chem Soc 1995;117:12855–60.

[4] Mizuguchi J, Honma S. Intermolecular charge transfer in 1,4-dithioketo-3,6-diphenyl-pyrrolo-[3,4-c]-pyrrole. J Appl Phys 1989;66:3104–10.

[5] Grifiths J. In this, the exploitable properties of dye chromophores are summarized and, they are light absorption, emission, light-induced polarization, photoelectric properties, and chemical and photochemical reactivities. Chemistry in Britain 1986:997.

[6] Matsuoka M, Oshida A, Mizoguchi A, Hattori Y, Nishimura A. Molecular design of quinoid dyes for 3rd order NLO materials. Nonlinear Optics 1995;10:109–14.

[7] Kim JH, Matsuoka M, Fukunishi K. Synthesis and solid state absorption spectra of some aminonaphthoquinone dyes. Dyes and Pigments 1996;31:263–72.

[8] Ramamurthy V, Venkatesan K. Photochemical reaction of organic crystals. Chem Rev 1987;87:433–81.

[9] Cohen MD, Schmidt GMJ. Topochemistry. Part I. J Chem Soc 1964;1996–2000.

[10] Begley MJ, Crombie L, Knapp TFWB. Topochemical controlled photo-dimerization of crystalline methyl 6-isobutenyl-2-methyl-4-oxocyclohex-2-ene-carboxylate: A chemical and X-ray crystallographic study. J Chem Soc Perkin I 1979;976–89.

[11] Addadi L, Cohen MD, Lahav, M. The synthesis of optical active dimers and polymers by reaction in crystals of chiral structure. J Chem Soc Chem Comm 1975;471–473.

[12] Addadi L, Mil JV, Lahav M. Engineering of chiral crystals for asymmetric ($2_\pi + 2_\pi$) photopolymerization. Execution of an "absolute" asymmetric synthesis with quantitative enantiomeric yield. J Am Chem Soc 1982;104:3422–9.

[13] Bates RB, Christensen KA, Hallberg A, Klenck RE, Martin AR. Solid- and liquid-phase photodimerizations of 5H-Indolo[1,7-*ab*][1]benzazepine. J Org Chem 1984;49:2978–81.

[14] Nakanishi F, Hasegawa M. Four-center type photopolymerization in the solid state. IV. Polymerization of α,α'-dicyano-*p*-benzenediacrylic acid and its derivatives. J Polym Sci A-1 1970;8:2151–60.

[15] Sarma JARP, Desiraju GR. The novel 1:1 donor-acceptor complex, 3,4-dimethoxycinnamic acid-2,4-dinitrocinnamic acid. Crystal engineering, structure, and anomalous lack of solid-state topochemical reactivity. J Chem Soc Perkin trans 2 1985:1905–12.

[16] Hasegawa M, Saigo K, Mori T, Uno H, Nohara M, Nakanishi H. Topochemical "double" photocyclodimerization of the 1,4-dicinnamoylbenzene crystal. J Am Chem Soc 1985;107:2788–93.

[17] Chung C, Hasegawa M. "Kaleidoscopic" photoreaction behavior of alkyl 4-[2-(4-pyridyl)ethenyl]cinnamate crystals: a crystalline linear high polymer from the methyl ester, an "absolute" asymmetric reaction of the ethyl ester, and two types of dimer formation from the propyl ester. J Am Chem Soc 1991;113:7311–6.

[18] Appel WK, Jiang ZQ, Scheffer JR, Walsh L. Crystal lattice control of unimolecular photorearrangements. Medium-dependent photochemistry of cyclohexenones. J Am Chem Soc 1983;105:5354–63.

[19] Ariel S, Askari S, Scheffer JR, Trotter J, Walsh L. Steric compression control of photochemical reactions in the solid state. J Am Chem Soc 1984;106:5726–8.

[20] Ito Y, Matsuura T, Tabata K, Ji-Ben M, Fukuyama K, Sasaki M, Okada S. Solid state photochemistry of methyl-substituted benzophenones. Tetrahedron 1987;43:1307–12.

[21] Ariel S, Askari S, Evans SV, Hwang C, Jay J, Scheffer JR, Trotter J, Walsh L, Wong Y. Reaction selectivity in solid state photochemistry. Tetrahedron 1987;43:1253–72.

[22] Bar I, Bernstein J. Conformational polymorphism. 4. Crystal energetics of a trimorphic system including disorder. J Phys Chem 1982;86:3223–31.

[23] Murthy GS, Arjunan P, Venkatesan K, Ramamurthy V. Consequences of lattice relaxability in solid state photodimerizations. Tetrahedron 1987;43:1225–40.

[24] Nakanishi F, Nakanishi H, Tsuchiya M, Hasegawa M. Water-participation in the crystalline-state photodimerization of cinnamic acid derivatives. A new type of organic photoreaction. Bull Chem Soc Jpn 1976;49:3096–9.

[25] Mizuguchi J, Rochat AC. A new near-infrared photoreceptor based on 1,4-dithioketo-3,6-diphenyl-pyrrolo-[3,4-c]-pyrrole. J Imaging Sci 1988;32:135–40.

[26] Zlatkevich L, Luminescence Techniques in Solid State Polymer Research. Marcel Dekker, New York, 1989

[27] Jaung JY, Matsuoka M, Fukunishi K. Syntheses and characterization of new styryl fluorescent dyes from DAMN. Part II. Dyes and Pigments 1997;34:255–66.